nzsee
NEW ZEALAND SOCIETY FOR EARTHQUAKE ENGINEERING

Chevron buckling restrained brace frame seismic behaviour considering out-of-plane effects

T.K.M. Simpson, A.J. Donald, G.A. MacRae
University of Canterbury, Christchurch, New Zealand.

ABSTRACT

This project evaluates the behaviour of buckling restrained braces (BRBs) in a chevron configuration considering in-plane (IP) and out-of-plane (OOP) frame deformations using software capable of second-order inelastic frame analysis. Initially a realistic single-storey, single-bay chevron BRB system was analysed. Performance was assessed to prevent buckling and undesirable system yielding. Previously published equations to predict yield were extended to also consider IP frame moment demands. Performance assessments then considered the following modifications: (a) a 'super-X' configuration, (b) increased gusset plate (GP) stiffnesses, (c) different beam configurations, and (d) a shortened casing length to account for flexibility at the casing ends.

For the initial chevron configuration, the ratio of the maximum brace force obtained according to the AISC provisions, C^*_{max}, to the system Euler buckling axial force, P_e, was 0.389, exceeding the allowable C^*_{max}/P_e of 0.285. The observed difference for the super-X configuration was insignificant compared to the initial chevron configuration. Increasing the GP stiffness decreased C^*_{max}/P_e to as low as 0.215, indicating that the GP governs the buckling behaviour. Cover plates at the beam tips, which increased the beam strength and stiffness, had little effect on the buckling force unless a high GP stiffness was also present. An OOP lateral restraint applied at the beam-brace joint had an insignificant effect on P_e when cover plates were provided. However, when no cover plates were provided, P_e decreased by 6.8%. Considering the initial chevron configuration with the casing length reduced at each end to consider gapping effects, C^*_{max}/P_e increased to 0.426. IP frame deformations could contribute as much as 25% to the GP section yield, so should not be ignored.

1 INTRODUCTION

A buckling restrained brace (BRB) can increase frame stiffness and dissipate earthquake energy. BRBs have become popular in the Christchurch rebuild, and like other new structural devices, are not specifically included in current NZ seismic standards. Rather, they are classified as an 'alternative solution' which must satisfy the intent of the NZ Building Code. Currently in New Zealand, the American Institute of Steel (AISC) design provisions are often used as evidence of compliance with the NZ Building Code. However, AISC testing requirements for BRBs do not consider the action of the brace as part of a frame, and generally only

consider axial loading. As a result, out-of-plane (OOP) frame deformations are typically not designed for, which may have a significant effect on BRB system performance.

Methods have been developed to ensure that diagonally braced BRB frames subject to in-plane (IP) and OOP cyclic deformations do not buckle, and do not yield outside the restrained BRB core, under the expected deformations. Similar considerations are not available for chevron BRB frames, where the beam lateral and rotational flexibility affects the moment demands. Therefore, there is a need to quantify demands and develop criteria to ensure that chevron BRB systems behave satisfactorily under expected IP and OOP deformations.

The objective of this study is to address the need by answering the following questions:

1. How should chevron BRB systems be modelled and analysed considering buckling and yield?
2. Should IP moment demands be considered for critical element yield, in addition to OOP moment and axial effects proposed in recent studies?
3. How do model configurations representing steel frames behave considering: (a) a single-storey chevron, (b) a two-storey super-X, (c) stiffened gusset plates, (d) beam cover plates, (e) beam lateral restraint, and (f) casing end rotational flexibility?

2 LITERATURE

2.1 Overall Considerations

Simple design recommendations have been developed for BRBs (MacRae et al., 2022). These consider OOP bending effects and they are provided with a design example by MacRae et al., (2023). The design approach is established so that yielding only occurs at the core yield zone, located within the casing of a BRB, rather than elsewhere in the BRB system. The approach, which uses simple interaction equations in a form with which engineers are familiar, is followed within this document as described below.

2.2 Gusset Plate Considerations

Often failure of BRB systems occurs due to buckling or yielding within the gusset plate (GP) region. MacRae et al. (2022) recommends that the GP is modelled as a single element, rather than using other approaches developed for bridge braces, where negative effective lengths can be obtained. To calculate the stiffness of an unstiffened GP element, it is assumed that the gusset plate element is made up of three sub-elements. The length of each sub-element is taken as the distance from the connection to the beam/column, as seen in Figure 1.

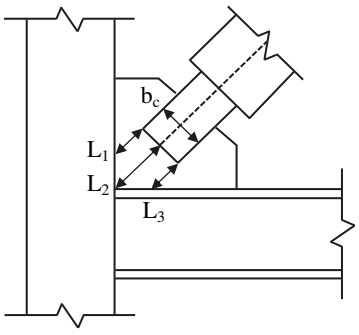

Figure 1: Gusset plate modelling approach

The section dimensions of each sub-element, i, are then given by a width of $b_c/2$ and the GP thickness. The OOP second moment of area for each sub-element, I_y, is input into Equation 1 to calculate the total OOP second moment of area for the GP element, $I_{y,GP}$, where L_{GP} is the GP element length:

$$I_{y,GP} = L_{GP}^2 \sum_i \frac{I_{y,i}}{L_i^2} \quad (1)$$

2.3 Flexibility at End of Casing

At the BRB casing ends, some rotational flexibility is expected. MacRae et al. (2021) suggests that this flexibility is either represented as a rotational spring, or as a reduced casing length, as seen in Figure 2. Unless better information is available, a lower bound stiffness is obtained by reducing the casing length by the casing diameter/width at each end of the casing.

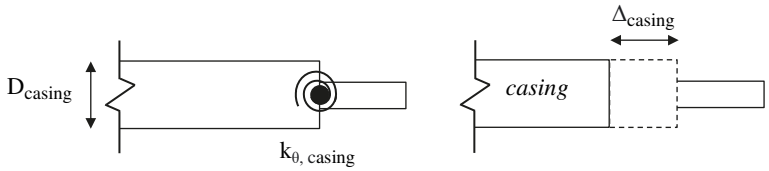

(a) Rotational spring *(b) Reduced casing length*

Figure 2: Methods for modelling casing ends

2.4 BRB System Axial Demand

Axial strength parameters for BRBs are obtained according to AISC360 Section F4.5b3 (2016). According to these provisions, BRBs are tested cyclically to twice the design ultimate limit state (ULS) displacement ($2\Delta_{ULS}$), and the axial forces at $2\Delta_{ULS}$ are taken as the axial capacities. The maximum compressive strength, C_{max}^*, is calculated using Equation 2, according to AISC341 F4-2a (2016). Here, P_{ysc} is the nominal yield strength of the BRB yielding core, R_y is the ratio of the measured actual yield strength to the nominal yield strength accounting for material variability (equivalent to ϕ_{om} in NZS3404 (1997) Clause 12.2.8), ω is the ratio of the peak measured tensile strength at $2\Delta_{ULS}$ to the nominal yield strength accounting for strain hardening, and β is the ratio of the measured peak compression strength to the peak tensile strength at $2\Delta_{ULS}$ to account for higher compressive forces.

$$C_{max}^* = \omega\beta R_y P_{ysc} \quad (2)$$

During seismic action, BRB frames are generally subject to bi-directional shaking. As a result, frame OOP deformations can cause the compressive strength to increase due to friction or gouging. MacRae et al. (2021) proposed to account for this increased axial force, $C_{max,o}^*$, using Equation 3. Here, γ is the ratio of compressive strength considering OOP and IP loading to that considering only IP loading. Experimental testing by Cui (2021) indicated that the compressive strength can increase by up to 30%. MacRae therefore recommends that γ be taken as 1.3 in the absence of more information.

$$C_{max,o}^* = \gamma\omega\beta R_y P_{ysc} \quad (3)$$

2.5 OOP Bending Demands

MacRae et al. (2022) has suggested that the BRB OOP moment demands on each element, M_{OOP}^*, can be obtained by conducting a second-order frame analysis to the expected OOP drift.

2.6 BRB System Axial Capacity

The BRB system elastic compressive strength, P_e, is dependent on all elements in the BRB system (Westeneng et al. 2015, and MacRae et al. 2022). P_e can be obtained for the brace via second-order elastic analysis of (a) the frame, or (b) the BRB system considering the brace as a single 'column' element, with end restraints obtained from a frame elastic analysis.

The BRB system nominal compressive strength, P_n, accounts for effects such as the buckling propensity, material non-linearity, and out-of-straightness. MacRae et al. (2021) suggest that this can be computed for each element, i, along the BRB system, in accordance with the axial compression member design approach with member slenderness, λ_n, obtained from NZS3404 (1997) Section 6.3.4b according to Equation 4. MacRae also suggests that the nominal compressive design stress be computed using the NZS3404 column curve for $\alpha_b = +0.5$.

$$\lambda_n = 90\sqrt{P_y/P_e} \tag{4}$$

2.7 BRB System Design Checks

The elastic buckling force, P_e, should satisfy Equation 5 which is equivalent to NZS3403 (1997) Clause 4.9.1 where $\lambda_c\ (= P_e/C^*_{max}) \geq 3.5$. This accounts for the possibility that C^*_{max} is significantly greater than expected (Cui 2021, and Dong et al. 2020), as well as other factors such as large out-of-straightness and residual stresses.

$$C^*_{max} < 0.285P_e \tag{5}$$

MacRae et al. (2022) suggests that Equation 6 is used for each element, i, along the BRB system length. This considers a linear moment-axial load interaction, where the strength reduction factor ϕ is taken as 0.9, and $M_{y,OOP}$ is the nominal OOP flexural strength of the section considered, calculated as the yield stress multiplied by the elastic section modulus.

$$\frac{C^*_{max,o}}{\phi P_{n_i}} + \frac{M^*_{OOP_i}}{\phi M_{y,OOP_i}} \leq 1 \tag{6}$$

3 METHODOLOGY

3.1 Structure Selection and Modelling Software

The structure selected for analysis was considered to represent a realistic chevron BRB frame. No slab is present, and the beam is provided with plates parallel to the web at both flange tips, increasing the beam strength and stiffness. Only one or two levels of frame are considered in the analyses below. Information about the modelling details and input files are given in the Appendix.

All analyses were conducted using the frame analysis software MASTAN2 (McGuire et al., 2000).

3.2 Design Checks

Equation 5 was used to check for axial buckling. Due to axial force alone, there is no OOP strength-increase factor so γ = 1.0. Here, P_e was found using a three-dimensional elastic critical buckling load analysis with a lateral force applied IP at a beam-column joint, with both beam-column joints restrained against OOP displacement.

For the yield check, a modification to Equation 6 is proposed in Equation 7 where IP demands are also explicitly considered in the yield evaluation. Here, $M_{y,IP}$ is the section nominal IP flexural strength, calculated similarly $M_{y,OOP}$. The IP flexural demand, M^*_{IP}, may be obtained at the prescribed IP displacement of $2\Delta_{ULS}$ (= 96 mm, or approximately 2% drift in the case considered). M^*_{OOP} is obtained in the same way by applying displacements at each beam-column joint, where the OOP drift in this direction is $2\Delta_{ULS}$ (or 84 mm). Second-order inelastic analyses were used to obtain the moment demands, using the predictor-corrector method with a force step of 0.01, as smaller force increments did not affect the results. Inelastic analysis accounts for the inelastic force demand in the brace core yield zone being lower than that if an elastic

analysis was performed, affecting the moment demands. Here, ϕ was taken as 1 as it was assumed material properties were known for the representative structure, while 0.9 should be used for design.

$$\frac{C^*_{max,o}}{\phi P_{n_i}} + \frac{M^*_{OOP_i}}{\phi M_{y,OOP_i}} + \frac{M^*_{IP_i}}{\phi M_{y,IP_i}} \leq 1 \tag{7}$$

3.3 Chevron BRB Reference Model

A reference model of a chevron BRB frame was modelled in three dimensions, as seen in Figure 3.

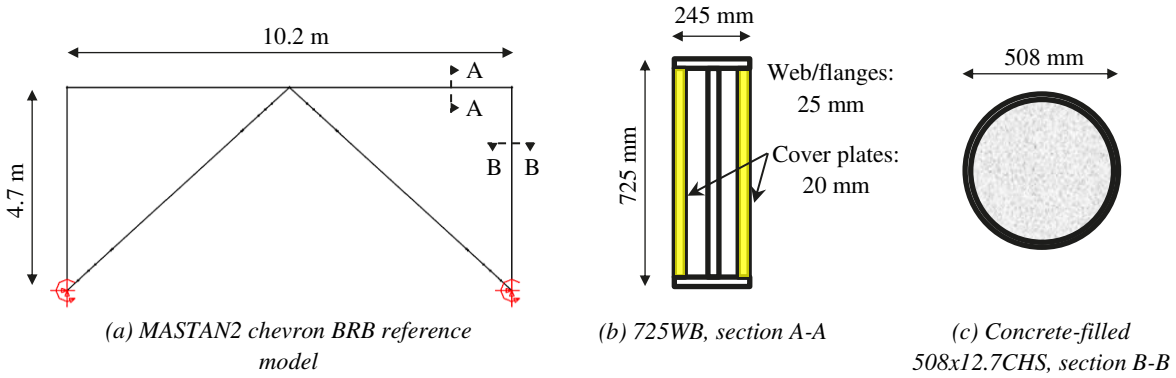

(a) MASTAN2 chevron BRB reference model

(b) 725WB, section A-A

(c) Concrete-filled 508x12.7CHS, section B-B

Figure 3: Chevron BRB reference model

The BRB members of the model were simplified into 11 elements, with length dimensions seen in Figure 4. The area, torsion constant, second moment of areas and the elastic section moduli were calculated for each element. The warping torsional constant was ignored, as it was found to have an insignificant effect on results. Element-to-element flexural connections were modelled as rigid to represent a high stiffness between elements. This included between the GPs and beam/columns, as GP-frame connections are welded.

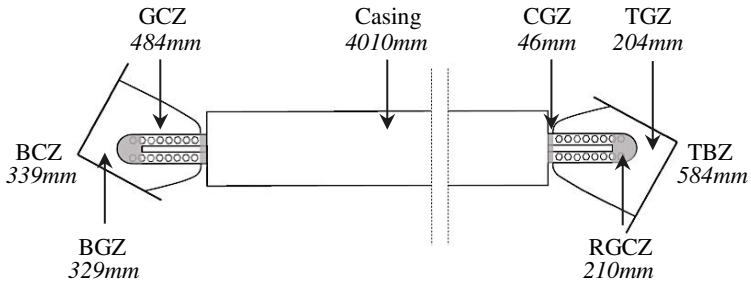

Figure 4: Components of a BRB member model

The bottom and top of the modelled BRB member consists of the bottom column zone (BCZ) and top beam zone (TBZ). The TBZ accounts for stiffeners at the beam-brace joints, and both the BCZ and TBZ account for the distance from the relevant gusset plate to the centroid of the column and beam, respectively. The section properties of the beam element computed were also applied to the TBZ. The BCZ section properties pertaining to stiffness were then modelled as ten times greater than the TBZ properties, to account for a high stiffness considering a concrete-filled column, while not being too high and potentially introducing numerical instability to the model. The base of the column was fixed for displacement and rotation in all axes assuming a rigid foundation.

Adjoining these zones are the bottom gusset zone (BGZ) and top gusset zone (TGZ), which are modelled according to Section 2.2. This is followed by a rounded gusset connection zone (RGCZ) and gusset

connection zone (GCZ). A connection gap zone (CGZ) is between the GCZ and the casing. The casing element simultaneously accounts for the yield strength of the core yield zone (CYZ) and the flexural stiffness of the concrete-filled steel restrainer. The CYZ yield strength was 290 MPa, while all steel elements other than the core had a yield strength of 350 MPa. The flexural stiffness of the casing only accounted for the steel restrainer, which used a 300 mm square cross-section. Realistic BRB system parameters were set as $P_{ysc} = 3555$ kN, $\omega\beta = 1.11$, and $R_y = 1.125$.

For simplicity, the length of the brace considered in analyses was taken at the frame initial, at-rest position, as opposed to the maximum or minimum extension. However, these could also be considered in design.

3.4 Modifications to Reference Model

Super-X Configuration

To investigate the effect of the strength in a Super-X configuration, an additional storey was placed on the frame as shown in Figure 5. Design checks were performed considering both $2\Delta_{ULS}$ displacements at the second level relative to the first level, and $2\Delta_{ULS}$ displacements at the first level.

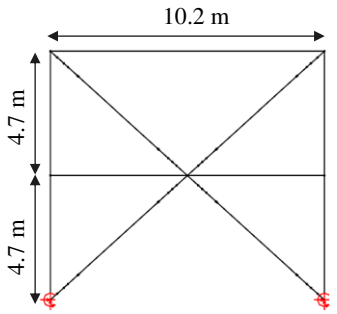

Figure 5: Super-X configuration

Different Gusset Plate Stiffnesses

A stiffener was added to the GP, as seen in Figure 6. From the unstiffened GP, the width of the stiffener was increased in 100 mm increments, to a width of 500 mm, excluding the GP width. This was performed considering a stiffener thickness, t_s, of both 32 mm and 64 mm.

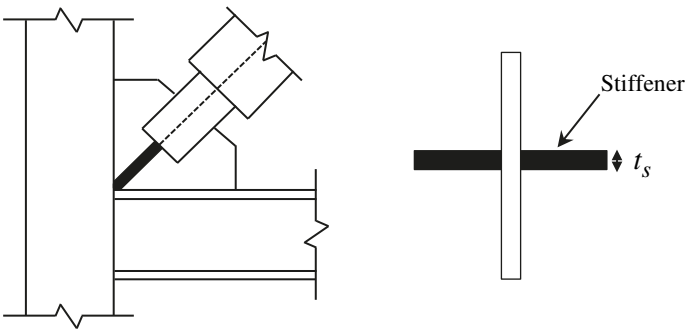

(a) Stiffened GP elevation *(b) Stiffened GP section*

Figure 6: Stiffened gusset plate

Different Beam Configurations

The beam section shown in Figure 3b was modified to also consider cover plate thicknesses of 0 mm (no cover plate), 10 mm, 40 mm, and 60 mm. The resulting beam stiffnesses were considered in conjunction with the different GP stiffnesses. Additionally, an OOP lateral restraint at the beam-brace joint was considered to observe the effect of this on P_e.

Reduced Casing Length

The casing length was reduced to represent a level of rotational flexibility at the casing ends, according to Section 2.3. Variations of this modification included reducing each end of the casing element by the width of the casing, half the width, and a quarter of the width, respectively. To assess the significance of this modification on the likely critical GP element, different GP stiffnesses were considered in conjunction with the reduced casing lengths. Reductions in casing length were replaced with a new element referred to as the connection end zone (CEZ), modelled according to the core profile at the casing ends.

4 BEHAVIOUR/FINDINGS

4.1 Chevron BRB Reference Model

Here, P_e was found to be 11,420 kN. Since C^*_{max} was computed as 4439 kN, C^*_{max}/P_e was found to be 0.389, greater than the allowed value of 0.285 for buckling in Equation 5. Table 1 shows the yield ratio, computed according to Equation 7, in relevant elements of the BRB member, all of which exceeded the allowed limit. The IP moment can be of significance to the yield ratio, as most notably seen in the bottom gusset zone, in which the contribution was 11.1%.

Table 1: Yield check results for reference model elements

Member ID	Yield Ratio	% of Yield Ratio due to IP Moment
Bottom Gusset Zone (BGZ)	2.5	11.1%
Rounded Gusset Connection Zone (RGCZ)	1.3	10.8%
Gusset Connection Zone (GCZ)	1.1	9.0%
Connection Gap Zone (CGZ)	1.2	1.3%
Connection Gap Zone (CGZ)	1.2	2.3%
Gusset Connection Zone (GCZ)	1.0	6.0%
Rounded Gusset Connection Zone (RGCZ)	1.2	8.7%
Top Gusset Zone (TGZ)	2.1	9.4%

4.2 Super-X Configuration

There was only a small difference in P_e comparing the Super-X configuration to the reference chevron model. This is reasonable considering that the critical buckling element between models remain the same. Yielding checks between the two models varied by no more than 3%.

4.3 Modified Gusset Plate Stiffness

Increasing the GP stiffness with stiffeners significantly increased P_e, causing acceptable C^*_{max}/P_e values, as seen in Figure 7, where 't_s' is the stiffener thickness. The GP was the system critical element considering

buckling. The stiffest GP configuration reached a C^*_{max}/P_e ratio of 0.215. Figure 8 shows the effect of GP stiffness on the GP yield ratio, considering the moment demands at $2\Delta_{ULS}$ IP and OOP. Only a larger stiffener size prevented the GP from yielding at these displacements. Here, the largest contribution to the GP yield ratio from the IP moment demand was 25%.

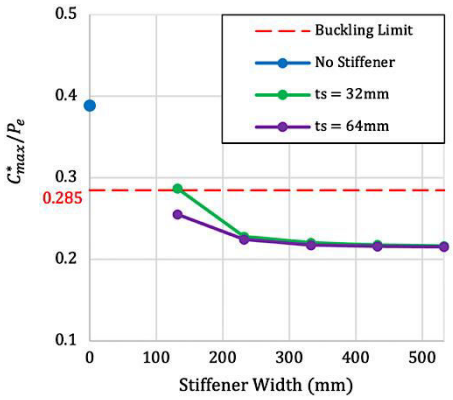

Figure 7: Buckling check for different stiffener sizes

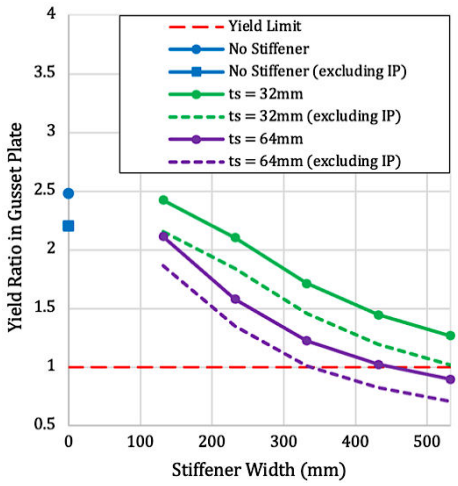

Figure 8: Yield ratio in GP for different stiffener sizes

Figure 9 displays the effect of OOP moment demands from OOP drift on the system yield check, considering yielding only occurring in the GP. An IP displacement of $2\Delta_{ULS}$ was applied simultaneously, and $C^*_{max,o}$ was considered for all OOP drifts. OOP moment demand increased with drift, and the yield ratio decreased considering larger stiffener sizes, allowing for larger OOP drifts before GP yield. The only GP that did not yield was the highly stiffened GP at drifts less than 1.5%.

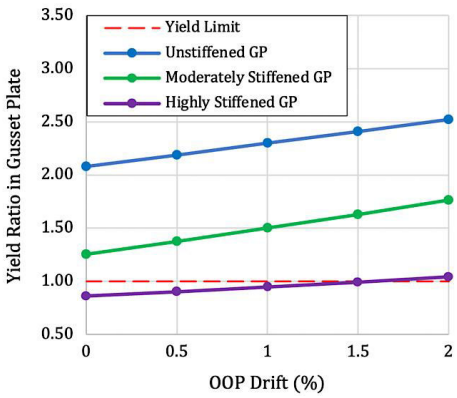

Figure 9: Yield ratio in GP considering OOP drift

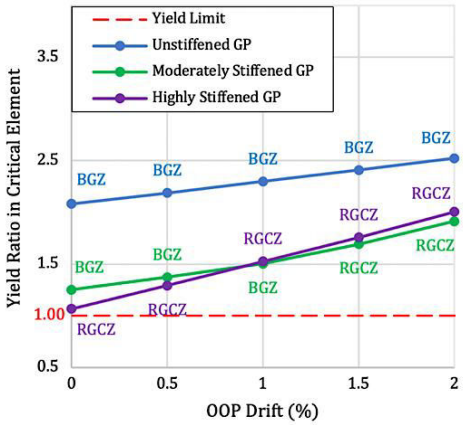

Figure 10: Yield ratio in critical element considering OOP drift

Increasing GP stiffness provided acceptable GP yield performance in this case. However, it can also result in increased moment demand that can cause other elements in the BRB system to govern the Equation 7 yield check, as shown in Figure 10. Due to a low yield area, GPs are the critical yielding elements when unstiffened, while connection zone elements are critical with a highly stiffened GP.

4.4 Modified Beam Configurations

Figure 11 shows the effect of cover plate thickness on P_e, considering different GP stiffnesses. When the cover plates are removed, the beam stiffness significantly decreases, as does P_e. The decrease in P_e becomes less significant as GP stiffness is increased, but it still does not satisfy the buckling check. However, the stability check can be satisfied with a highly stiffened GP and a thick cover plate.

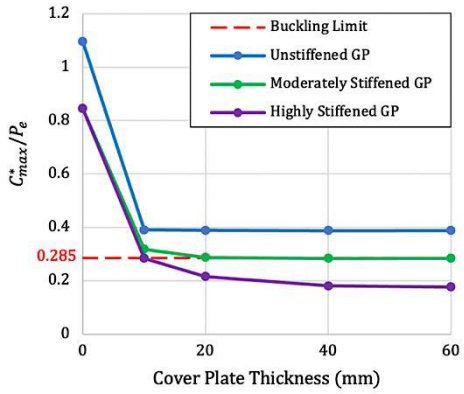

Figure 11: Buckling check for different cover plate thicknesses

For the reference chevron model, which uses a cover plate thickness of 20 mm, the effect of lateral restraint, at the mid-length of the beam changed P_e by only 0.1%. However, if no cover plates are used, the lateral restraint increases P_e by 6.8%.

4.5 Reduced Casing Length

Figure 12 shows that as casing length decreases (i.e. the casing reduction increases), implying greater end zone flexibility, the P_e decreases, causing greater C^*_{max}/P_e, with a maximum value of 0.426. The effect of casing length on C^*_{max}/P_e decreases with GP stiffness, with none observed for a high GP stiffness.

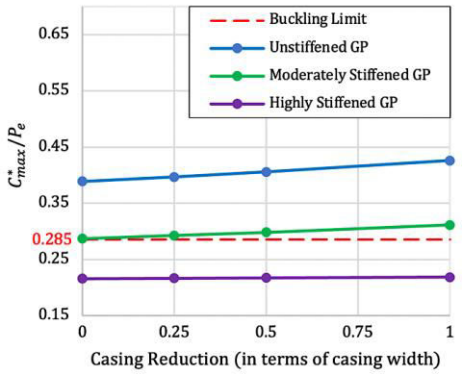

Figure 12: Buckling check for casing reductions

5 CONCLUSIONS

The behaviour of buckling restrained braces was evaluated in a chevron configuration considering IP and OOP frame deformations. It was found that:

1. A three-dimensional model of the chevron BRB system could be modelled using software capable of second-order inelastic frame analysis, such as MASTAN2. The Euler buckling load, P_e, and the IP and OOP moment demands could be obtained from this model.
2. IP moment demands contributed up to 25% of the critical element yield, and thus should be included, in addition to axial demands and OOP moment demands, when assessing system yield.
3. The system buckling ratio (C^*_{max}/P_e) limit of 0.285, and the yield limit (from Equation 7) of 1.0 was checked. For the cases analysed it was found that the critical yield ratio occurred in the gusset plate, and:
   a. the reference model (i.e. single-storey chevron BRB) C^*_{max}/P_e ratio was 0.389 (failing the system buckling limit), and the Equation 7 system yield check was also not satisfied,
   b. the Super-X model behaved similarly to the reference model, with critical ratios differing by < 3%,
   c. stiffened gusset plates increased the system elastic buckling capacity, P_e, providing an acceptable C^*_{max}/P_e ratio as low as 0.215. Larger GP stiffeners also prevented GP yielding, but caused other end zone elements to increase in yield ratio and govern the yield check,
   d. beam cover plate size increase only increased C^*_{max}/P_e for small cover plate thickness,
   e. beam mid-length OOP (i.e. lateral) restraint increased P_e by 6.8% when no cover plates were provided, but did not affect P_e otherwise, and
   f. modelling end of casing flexibility, by reducing the casing length, increased the reference model C^*_{max}/P_e to 0.426. However when highly stiffened GPs were used, changes were insignificant.

6 ACKNOWLEDGEMENTS

The authors would like to express gratitude to Reagan Chandramohan for assistance with modelling queries.

7 REFERENCES

AISC (American Institute of Steel Construction). 2016. *Seismic Provisions for Structural Steel Buildings.* AISC 341-16. Chicago, Illinois

AISC (American Institute of Steel Construction). 2016. *Specification for Structural Steel Buildings.* AISC 360-16.

Cui, J. (2021). "BRB performance issues. " University of Canterbury.

Dong, W., Li, M., Lee, C-L., MacRae, G. A., and Abu, A. (2020). "Experimental testing of full-scale glulam frames with buckling restrained braces." *Engineering Structures*, 222(1).

MacRae, G.A., Lee, C-L., Vazquez-Colunga, S.Y., Cui, J., Alizadeh, S., and Jia, L-J. (2021). "BRB system design for stability." *Bulletin of the New Zealand Society for Earthquake Engineering*, 54(1).

MacRae G.A., Lee C-L, Vazquez-Colunga S. Y, Cui J., Alizadeh S., and Jia L-J., "BRB System Design for Out of Plane Deformations", Steel Structures in Seismic Areas (STESSA) Conference, Timisoara, Romania, 25-27 May 2022.

MacRae, G. A., Lee, C-L., Vazquez-Colunga, S.Y., Cui, J., and Jia, L-J. (2023). "BRB system design considerations." *New Zealand Society for Earthquake Engineering*, submitted for publication.

McGuire W, Gallagher R. H., Ziemian R. D. (2000). *Matrix Structural Analysis, 2nd Edition,* Bucknell Digital Commons, Faculty Books 7.

NZS (Standards New Zealand). 1997. *Steel Structures Standard.* NZS 3404:Part 1:1997.

Westeneng, B., Lee, C-L., MacRae, G. A., Jones, A. (2015). "Out-of-plane buckling behaviour and design of BRB gusset plate connections."

8 APPENDIX

The Dropbox link below directs to Excel spreadsheets and MASTAN2 models containing information about the modelling details and input files:

https://www.dropbox.com/scl/fo/kywivlu76ccatxht0eoyw/h?dl=0&rlkey=ltfuae97pjh4irpgvee3p1605